Chapter

G-Jitter Effects on Chaotic Convection in a Rotating Fluid Layer

Palle Kiran

Abstract

The effect of gravity modulation and rotation on chaotic convection is investigated. A system of differential equation like Lorenz model has been obtained using the Galerkin-truncated Fourier series approximation. The nonlinear nature of the problem, i.e., chaotic convection, is investigated in a rotating fluid layer in the presence of g-jitter. The NDSolve Mathematica 2017 is employed to obtain the numerical solutions of Lorenz system of equations. It is found that there is a proportional relation between Taylor number and the scaled Rayleigh number R in the presence of modulation. This means that chaotic convection can be delayed (for increasing value of R) or advanced with suitable adjustments of Taylor number and amplitude and frequency of gravity modulation. Further, heat transfer results are obtained in terms of finite amplitude. Finally, we conclude that the transition from steady convection to chaos depends on the values of Taylor number and g-jitter parameter.

Keywords: g-jitter effect, nonlinear theory, rotation, chaos, truncated Fourier series

1. Introduction

The study of chaotic convection is of great interest due to its applications in thermal and mechanical engineering and in many other industry applications. It was introduced by Lorenz [1] to illustrate the study of atmospheric three-space model arising from Rayleigh-Benard convection. Some of the applications are production of crystals, oil reservoir modeling, and catalytic packed bed filtration. He developed a simplified mathematical model for atmospheric convection given below:

$$x' = Pr(y - x), \tag{1}$$

$$y' = x(R - z) - y, \tag{2}$$

$$z' = xy - \beta z. \tag{3}$$

This model is a system of three ordinary differential equations known as the Lorenz equations. These equations are related to the properties of a two-dimensional Rayleigh-Benard convection. In particular, the system describes the rate of change of three quantities convection, temperature variation vertically with respect to time. These equations are related to the properties of two-dimensional

flow model warmed uniformly from below and cooled from above. In particular, the system describes the rate of change of three quantities of time, x is proportional to the rate of convection, y is the horizontal temperature variation, and z is the vertical temperature variation. The constants Pr, R and β are the system parameters proportional to the Prandtl number, Rayleigh number, and certain physical dimensions of the media. If $R < 1$ then there is only one equilibrium point at the origin which is represented as no convection point. Further, all orbits converge to the origin, which is a global attractor. When R = 1, then a pitchfork bifurcation occurs, and for R_1, two additional critical points arise and are known as convection points, and there the system loses its stability. In addition to this model, I would like to add the concept of modulation either to suppress or to enhance nonlinearity. The literature shows that there are different types available; some of them are temperature modulation (Venezian [2]), gravity (Gresho and Sani [3] and Bhadauria and Kiran [4, 5]), rotation (Donnelly [6], Kiran and Bhadauria [7]), and magnetic field modulation (Bhadauria and Kiran [8, 9]). Their studies are mostly on thermal convection either considering fluid or porous medium. Their ultimate idea behind the research is to find external regulation to the system to control instability and measure the heat mass transfer in the system. But what happens when we consider the external configuration to system Eq. (1). The external configurations are like thermal, gravity, rotation, and magnetic field modulation. In this direction, no data are reported so far. With this, I would like to extend the work of Lorenz along with modulation.

The studies on chaos with respect to the different types of parameters like Rayleigh number and Prandtl number are mostly investigated by the following studies. The transition from steady convection to chaos occurs by a subcritical Hopf bifurcation producing a solitary cycle which may be associated with a homoclinic explosion for low Prandtl number is investigated by Vadasz and Olek [10]. The work of Vadasz [11] suggests an explanation for the appearance of this solitary limit cycle via local analytical results. The effect of magnetic field on chaotic convection in fluid layer is investigated by Mahmud and Hasim [12]. They found that transition from chaotic convection to steady convection occurs by a subcritical Hopf bifurcation producing a homoclinic explosion which may limit the cycle as Hartman number increases. For the moderate values of Prandtl number, the route to chaos occurs by a period of doubling sequence of bifurcations given by Vadasz and Olek [13]. Feki [14] proposed a new simple adaptive controller to control chaotic systems. The constructed linear structure of controller may be used for chaos control as well as for chaotic system synchronization. Yau and Chen [15] found that the Lorenz model could be stabilized, even in the existence of system external distraction. For non-Newtonian fluid case, Sheu et al. [16] have shown that stress relaxation tends to accelerate onset chaos. A weak nonlinear solution to the problem is assumed by Vadasz [17], and it can produce an accurate analytical expression for the transition point as long as the condition of validity and consequent accuracy of the latter solution is fulfilled. Narayana et al. [18] investigated heat mass transfer using truncated Fourier series method. They have also discussed chaotic convection under the effect of binary viscoelastic fluids. The studies related to gravity modulation are given by Kiran et al. [19–25]. These studies show that the gravity modulation can be used to control heat and mass transfer in the system in terms of frequency and amplitude of modulation.

The above paragraph demonstrated the earlier work on chaotic convection with different configurations and models to control chaos. Recently Vadasz et al. [26] and Kiran et al. [27] have investigated the effect of vertical vibrations and temperature modulation on chaos in a porous media. Their results show that periodic solutions and chaotic solutions alternate as the value of the scaled Rayleigh number changes in the presence of forced vibrations. The root to chaos is also affected by three types of thermal modulations.

The effect of rotation on chaos is investigated by Gupta et al. [28] without any modulation. They found that rotation has delay in chaos and controls nonlinearity. It is also concluded that there are suitable ranges over Ta and R to reduce chaos in the system. Based on the above studies in this chapter, I would like to investigate the study of chaotic convection in the presence of rotation and gravity modulation.

2. Mathematical model

An infinitely extended horizontal rotating fluid layer about its vertical z-axis is considered. The layer is gravity modulated and the lower plate held at temperature T_0 while the upper plate at $T_0 + \Delta T$. Here ΔT is the temperature difference in the medium. The mathematical equation of the flow model is given by

$$\nabla . q = 0, \tag{4}$$

$$\frac{\partial \overline{q}}{\partial t} + 2\Omega * \overline{q} = -\frac{1}{\rho_0}\nabla p + \frac{\rho}{\rho_0}\overline{g} + \nu\Delta^2\overline{q}, \tag{5}$$

$$\frac{\partial T}{\partial t} + (\overline{q}.\nabla)T = k_T\nabla^2 T, \tag{6}$$

$$\rho = \rho_0[1 - \alpha_T(T - T_0)]. \tag{7}$$

The thermal boundary conditions are given by

$$T = T_0 + \Delta T \quad at \quad z = 0 \quad and \quad T = T_0 \quad at \quad z = d, \tag{8}$$

where $\overline{q} - >$ is the velocity of the fluid, $\Omega - >$ is the vorticity vector, $p - >$ is the fluid pressure, $\rho - >$ is the density, $\nu - >$ is the kinematic viscosity, $K_T - >$ is the thermal diffusivity ratio, and $\alpha_t - >$ is the thermal expansion coefficient. We consider in our problem the externally imposed gravitational field (given by Gresho and Sani [3]):

$$\vec{g} = g_0\left[1 + \delta_g \sin\left(\omega_g t\right)\right]\hat{k}, \tag{9}$$

where δ_g, ω_g are the amplitude and frequency of gravity modulation.

2.1 Basic state

The basic state of the fluid is quiescent and is given by

$$q_b = (0, 0, 0), p = p_b(z), T = T_b(z). \tag{10}$$

Using the basic state Eq. (10) in the Eqs. (4)–(6), we get the following relations

$$\frac{\partial \overline{q}_b}{\partial t} + 2\Omega * \overline{q}_b = -\frac{1}{\rho_0}\nabla p_b + \frac{\rho_b}{\rho_0}\overline{g} + \nu\Delta^2\overline{q}_b, \tag{11}$$

$$o = -\frac{1}{\rho_0}\nabla p_b + \frac{\rho_b}{\rho_0}\overline{g}, \tag{12}$$

$$\nabla p_b = \rho_b\overline{g}, \tag{13}$$

$$\frac{\partial p_b}{\partial z} = \rho_b\overline{g}, \tag{14}$$

and from Eq. (6)

$$\frac{\partial T_b}{\partial t} + (\overline{q}_b.\nabla)T = k_T\nabla^2 T_b, \tag{15}$$

$$k_T\nabla^2 T_b = 0, \tag{16}$$

$$T_b = T_0 + \Delta T\left(1 - \frac{z}{d}\right). \tag{17}$$

2.2 Perturbed state

On the basic state, we superpose perturbations in the form

$$q = q_b + q', \rho = \rho_b(z) + \rho', p = p_b(z) + p', T = T_b(z) + T' \tag{18}$$

where the primes denote perturbed quantities. Now substituting Eq. (18) into Eqs. (4)–(7) and using the basic state solutions, we obtain the equations governing the perturbations in the form

$$\nabla.\overline{q}' = , 0 \tag{19}$$

$$\frac{\partial(T_b + T')}{\partial t} + \left((q_b + q').\Delta\right)(T_b + T') = K_T\nabla^2(T_b + T'), \tag{20}$$

$$\frac{\partial T'}{\partial t} + (q'.\nabla)(T_b + T') = K_T\nabla^2(T'), \tag{21}$$

$$\frac{\partial T'}{\partial t} + \left(u'\frac{\partial}{\partial x} + w'\frac{\partial}{\partial z}\right)(T_b + T') = K_T\nabla^2(T'), \tag{22}$$

simplifying the above equation, then we get

$$\frac{\partial T'}{\partial t} - \frac{\partial\psi}{\partial x}\frac{\partial T_b}{\partial z} + \frac{\partial(\psi, T')}{\partial(x, z)} = K_T\nabla^2(T'). \tag{23}$$

Similarly we can derive the same for momentum equation of the following form

$$\frac{\partial\overline{q}'}{\partial t} + 2\Omega * \overline{q}' = -\frac{1}{\rho_0}\nabla p' + \frac{\rho'}{\rho_0}\overline{g} + \nu\Delta^2\overline{q}'. \tag{24}$$

We consider only two-dimensional disturbances and define the stream functions ψ and $\overline{q}$ by

$$(u', w') = \left(-\frac{\partial\psi}{\partial z}, \frac{\partial\psi}{\partial x}\right), \overline{g} = (0, 0, -g), \tag{25}$$

which satisfy the continuity Eq. (19). While introducing the stream function ψ and non-dimensionalizing with the following nondimensional parameters (x′,y′,z′) = d(x^*, y^*, z^*), t′ = $\frac{d^2}{K_T}t^*$, $T' = (\Delta T)T^*$, and $p' = \frac{\mu K_T}{d^2}p^*$, then the resulting Eq. (19) becomes

$$\frac{\partial T'}{\partial t} - \frac{\partial\psi}{\partial x}\frac{\partial T_b}{\partial z} + \frac{\partial(\psi, T')}{\partial(x, z)} = K_T\nabla^2(T'),$$

after simplifying the above equation, we get

$$\left(\frac{\partial}{\partial t}-\nabla^2\right)T=\frac{\partial\psi}{\partial x}-\frac{\partial(\psi,T)}{\partial(x,z)}. \tag{26}$$

Similarly while eliminating the pressure term and using the dimensionless quantities, from the momentum equation (24), we get the following:

$$\left[\left(\frac{1}{Pr}\frac{\partial}{\partial t}-\nabla^2\right)^2\nabla^2+T_a\frac{\partial^2}{\partial z^2}\right]\frac{\partial\psi}{\partial x}=Ra\left(1+\delta_g\sin\left(\omega_g t\right)\right)\frac{\partial^2}{\partial x^2}\left(\frac{1}{Pr}\frac{\partial}{\partial t}-\nabla^2\right)T, \tag{27}$$

where Pr = $\frac{\nu}{K_T}$ is the Prandtl number, $T_a=\frac{4d^4\Omega^2}{\nu^2}$ is the Taylor number, and $Ra=\frac{\alpha(\Delta T)d^3g_0}{\nu K_T}$ is the Rayleigh number. The assumed boundaries are stress free and isothermal; therefore, the boundary conditions are given by

$$w=\frac{\partial^2 w}{\partial z^2}=T=0\quad at\quad z=0\quad and\quad z=1. \tag{28}$$

The set of partial differential Eqs. (26) and (27) forms a nonlinear coupled system of equations involving stream function and temperature as a function of two variables in x and z. We solve these equations by using the Galerkin method and using Fourier series representation.

3. Truncated Galerkin expansion

To obtain the solution of nonlinear coupled system of partial differential equations (26) and (27), we represent the stream function and temperature in the form

$$\psi=A_1\sin(ax)\sin(\pi z), \tag{29}$$

$$T=B_1\cos(ax)\sin(\pi z)+B_2\sin(2\pi z) \tag{30}$$

The above are the Galerkin expansion of stream function and temperature. Now substituting these equations in Eqs. (26) and (27) and applying the orthogonal conditions to Eqs. (30) and (31) and finally integrating over the domain [0,1] × [0,1] yield a set of equations:

$$\frac{\partial B_1}{\partial t}\cos ax\sin\pi z+\frac{\partial B_2}{\partial t}\,sin\,2\pi z+k^2B_1\cos ax\sin\pi z+4B_2\pi^2\sin 2\pi z \tag{31}$$

$$=A_1a\cos ax\sin\pi z-A_1B_1a\pi\cos\pi z\sin\pi z \tag{32}$$

$$-2A_1B_2a\pi\cos 2\pi z\cos ax\sin\pi z. \tag{33}$$

Now multiply with $\cos ax\sin\pi z$ on both sides, and apply integration from 0 to 1 with respect to x and 0 to $\frac{2\pi}{a}$:

$$\frac{\partial B_1}{\partial t}\int_0^1\int_0^{\frac{2\pi}{a}}\cos^2 ax\sin^2\pi z dx dz+\frac{\partial B_2}{\partial t}\int_0^1\int_0^{\frac{2\pi}{a}}\cos ax\sin\pi z\sin 2\pi z dx dz \tag{34}$$

$$+k^2B_1\int_0^1\int_0^{\frac{2\pi}{a}}\cos^2 ax\sin^2\pi z dx dz \tag{35}$$

$$+4B_2\pi^2\int_0^1\int_0^{\frac{2\pi}{a}} sin\,2\pi z\cos ax\sin\pi z dxdz \tag{36}$$

$$= A_1 a\int_0^1\int_0^{\frac{2\pi}{a}}\cos^2 ax\sin^2\pi z dxdz \tag{37}$$

$$-A_1B_1a\pi\int_0^1\int_0^{\frac{2\pi}{a}}\cos ax\cos\pi z\sin^2\pi z dxdz \tag{38}$$

$$-2A_1B_2a\pi\int_0^1\int_0^{\frac{2\pi}{a}}\cos 2\pi z\cos^2 ax\sin^2\pi z dxdz. \tag{39}$$

$$\frac{\partial B_1}{\partial t}\frac{\pi}{2a}+k^2B_1\frac{\pi}{2a}=A_1a\frac{\pi}{2a}-2A_1B_2a\pi\left(-\frac{\pi}{2a}\right), \tag{40}$$

$$\frac{\partial B_1}{\partial t}=A_1a+A_1B_2a\pi-k^2B_1. \tag{41}$$

Now we consider $\tau = k^2t \Rightarrow t = \frac{\tau}{k^2}$.

$$\frac{\partial B_1}{\partial \tau}=\frac{A_1a}{k^2}+\frac{a\pi}{k^2}A_1B_2-B_1. \tag{42}$$

Now let us consider Eq. (30) and multiply with $sin\,2\pi z$ on both sides of the equation and apply integration from 0 to 1 with respect to x and 0 to $\frac{2\pi}{a}$:

$$\frac{\partial B_1}{\partial t}\int_0^1\int_0^{\frac{2\pi}{a}}\cos ax\sin\pi z sin2\pi z dxdz+\frac{\partial B_2}{\partial t}\int_0^1\int_0^{\frac{2\pi}{a}}\sin^2 2\pi z dxdz \tag{43}$$

$$+k^2B_1\int_0^1\int_0^{\frac{2\pi}{a}}\cos ax\sin\pi z\sin 2\pi z dxdz \tag{44}$$

$$+4B_2\pi^2\int_0^1\int_0^{\frac{2\pi}{a}}\sin^2 2\pi z dxdz \tag{45}$$

$$= A_1a\int_0^1\int_0^{\frac{2\pi}{a}}\cos ax\sin\pi z\sin 2\pi z dxdz \tag{46}$$

$$-\int_0^1\int_0^{\frac{2\pi}{a}}-\int_0^1\int_0^{\frac{2\pi}{a}}A_1B_1a\pi\cos\pi z\sin\pi z\sin 2\pi z dxdz \tag{47}$$

$$-\int_0^1\int_0^{\frac{2\pi}{a}}2A_1B_2a\pi cos2\pi z\cos ax\sin\pi z sin\,2\pi z dxdz, \tag{48}$$

then by simplifying the above equation, we get

$$\frac{\partial B_2}{\partial \tau}=-\frac{4\pi^2}{k^2}B_2-\frac{a\pi}{2k^2}A_1B_1. \tag{49}$$

Similarly from Eq. (50)

$$\frac{\partial^2 A_1}{\partial \tau^2} = -2Pr\frac{\partial A_1}{\partial \tau} + \frac{a}{K^6}\left(a^2 Ra\left(1+\delta_g \sin\left(\omega_g t\right)\right) - \pi^2 T_a Pr - k^6 Pr\right)A_1 + \frac{\pi a^2 PrRa}{k^6}A_1 B_2 + \frac{aRaPr(Pr-1)}{k^4}B_1, \tag{50}$$

where $k^2 = \pi^2 + a^2$ is the total wavenumber and $\tau = k^2 t$ is the rescaled time. Introducing the following dimensionless quantities

$$R = \frac{a^2 Ra}{K^6}, T = \frac{\pi^2 T_a}{k^6} \; and \; \gamma = -\frac{4\pi^2}{k^2}, \sigma = Pr, \tag{51}$$

and rescale the amplitudes in the form of

$$X = \frac{\pi a}{k^2\sqrt{2}}A_1, Y = \frac{\pi R}{\sqrt{2}}B_1 \quad \text{and} \quad Z = -\pi R B_2. \tag{52}$$

To provide the following set of equations, we consider the following equations $\gamma = -\frac{4\pi^2}{k^2}$, $\frac{1}{k^2} = -\frac{\gamma}{4\pi^2}$

$$\frac{\partial B_1}{\partial \tau} == \frac{\gamma a}{4\pi^2}A_1 - \frac{\gamma a \pi}{4\pi^2}A_1 B_2 - B_1, \tag{53}$$

$$\frac{\partial}{\partial \tau}\left(\frac{Y\sqrt{2}}{\pi R}\right) = \frac{\gamma aR}{4\pi^2}\left(\frac{Xk^2\sqrt{2}}{\pi aR}\right) - \frac{\gamma a}{4\pi}\left(\frac{Xk^2\sqrt{2}}{\pi a}\right)\left(-\frac{z}{\pi R}\right) - \frac{Y\sqrt{2}}{\pi R}, \tag{54}$$

and then simplifying the above equation, we get

$$Y' = RX - XZ - Y, \tag{55}$$

now from the Eq. (50)

$$\frac{\partial B_2}{\partial \tau} = \gamma B_2 - \frac{1}{2}\left(-\frac{\gamma}{4\pi^2}\right)\pi a A_1 B_1, \tag{56}$$

$$\frac{\partial}{\partial \tau}\left(\frac{Z}{\pi R}\right) = \gamma\left(\frac{z}{\pi R}\right) - \frac{1}{2}\left(-\frac{\gamma}{4\pi^2}\right)\pi a\left(\frac{Xk^2\sqrt{2}}{\pi R}\right)\left(\frac{Y\sqrt{2}}{\pi R}\right), \tag{57}$$

$$Z' = \gamma Z + XY. \tag{58}$$

Similarly from Eq. (28),

$$X' = W, \tag{59}$$

$$W' = -2\sigma w + \sigma\left(R\left(1+\delta_g \sin\left(\omega_g t\right)\right) - \sigma(T+1)\right)X - \sigma XZ + \sigma(\sigma-1)Y, \tag{60}$$

where the symbol (/) denotes the time derivative $\frac{d()}{d\tau}$. Eqs. (56), (59), and (61) are like the Lorenz equations (Lorenz (13), sparrow (14)), although with different coefficients. The final nonlinear differential equations are given by

$$X' = W, \tag{61}$$

$$Y' = RX - XZ - Y, \tag{62}$$

$$Z' = \gamma Z + XY, \tag{63}$$

$$W' = -2\sigma W + \sigma\left(R\left(1 + \delta_g \sin\left(\omega_g \tau\right)\right) - \sigma(T+1)\right)X - \sigma XZ + \sigma(\sigma - 1)Y. \tag{64}$$

4. Stability analyses

To understand the stability of the system, we determine the fixed points of the system and will try to find the nature of these fixed points through eigen equation. The nonlinear dynamics of Lorenz-like system (62)–(65) has been analyzed and solved for σ = 10, $\gamma = -\frac{8}{3}$ corresponding to convection. The basic properties of the system to obtain the eigen function are described next.

4.1 Dissipation

The system of Eqs. (62)–(65) is dissipative since

$$\nabla V = \frac{\partial X'}{\partial X} + \frac{\partial Y'}{\partial Y} + \frac{\partial Z'}{\partial Z} + \frac{\partial W'}{\partial W} = -(2\sigma + 1 - \gamma) < 0. \tag{65}$$

If the set of initial solutions is the region of V(0), then after some time t, the endpoints of the trajectories will decrease to a volume:

$$V(t) = V(0)\, exp\,[-(2\sigma + 1 - \gamma)t]. \tag{66}$$

The above expression shows that the volume decreases exponentially with time.

4.2 Equilibrium points

System (62)–(65) has the general form, and the equilibrium (fixed or stationary) points are given by:

$$X' = W, \tag{67}$$

$$W = 0. \tag{68}$$

From Eq. (83) we got

$$X = \frac{Y}{R - Z}, \tag{69}$$

and similarly we also got the following from Eq. (64):

$$Z = \frac{-Y^2}{\gamma(R - Z)}, \tag{70}$$

and similarly we also got the following from Eq. (65) for the momentum case:

$$R = T + 1, \tag{71}$$

then we get a relation

$$X_{2,3} = \pm \quad \frac{\sqrt{(T+1-R)\gamma}}{\sqrt{T+1}} \tag{72}$$

the remaining $Y_{2,3}, Z_{2,3}$ will be accessed. The fixed points of rescaled system for modulated case are $(X_1, Y_1, Z_1) = (0, 0, 0)$ corresponding to the motionless solution and $(X_{2,3}, Y_{2,3}, Z_{2,3}) = \left[\pm\sqrt{\frac{Z}{c}}, \pm c\sqrt{\frac{Z}{c}}, \frac{(RI_1-c)}{(R-1)^2}\right]$ corresponding to the convection solution. The critical value of R, where the motionless solution loses their stability and the convection solution takes over, is obtained as $R_{cr} = \frac{c}{I_1}$, which corresponds to $Ra = 4\pi^2 \frac{c}{I_1}$ where $c = \left(1 + C\frac{\pi^2}{\gamma}\right)$ and $I_1 = \int_0^1 \sin^2(\pi z) f_2 dz$. This pair of equilibrium points is stable only if $R < \sqrt{\frac{Z}{c}}$; beyond this condition the other periodic, quasi-periodic, or chaotic solutions take over at $R > \sqrt{\frac{Z}{c}}$. The corresponding stability of the fixed points associated with the motionless solution $(X_1, Y_1, Z_1) = (0, 0, 0)$ is controlled by the zeros of the following characteristic polynomial:

5. Stability of equilibrium points

The Jacobian matrix of Eqs. (62)–(65) is as follows:

$$J = DF_{(X,Y,Z,W)} = \begin{bmatrix} 0 & 0 & 0 & 0 \\ R-Z & -1 & -X & 0 \\ Y & X & \gamma & 0 \\ \sigma[R-\sigma(T+1)-Z] & \sigma(\sigma-1) & -\sigma X & -2\sigma \end{bmatrix}.$$

The characteristic values of the above Jacobian matrix, obtained by solving the zeros of the characteristic polynomial, provide the stability conditions. If all the eigenvalues are negative, then the fixed point is stable (or in the case of complex eigenvalues, they have negative real parts) and unstable, when at least one eigenvalue is positive (or in the case of complex eigenvalues, it has positive real part):

$$DF_{(0,0,0,0)} = \begin{bmatrix} 0 & 0 & 0 & 0 \\ R & -1 & 0 & 0 \\ 0 & 0 & \gamma & 0 \\ \sigma[R-\sigma(T+1)] & \sigma(\sigma-1) & 0 & -2\sigma \end{bmatrix}.$$

The characteristic equation for the above system at origin is given by $|A - \lambda I| = 0$ which implies the following

$$\gamma = \lambda, \lambda^3 + (2\sigma+1)\lambda^2 + \left[(2-R)\sigma + \sigma^2(T+1)\right]\lambda + \sigma^2(T-R+1) = 0.$$

The first eigenvalue γ is always negative as $\gamma = \frac{-8}{3}$, but the other three eigenvalues are given by equation

$$\lambda^3 + (2\sigma + 1)\lambda^2 + \left[(2 - R)\sigma + \sigma^2(T + 1)\right]\lambda + \sigma^2(T - R + 1) = 0.$$

The stability of the fixed points corresponding to the convection solution $(X_{2,3}, Y_{2,3}, Z_{2,3})$ is controlled by the following equation for the eigenvalues $\lambda_i, = 1, 2, 3, 4$:

$$\lambda^4 + \lambda^3(2\sigma + 1 - \gamma) + \lambda^2\left(2\sigma - \gamma - 2\gamma\sigma\gamma - \sigma T + \sigma^2 T - \sigma + \sigma^2 + X^2\right) + \lambda\left(X^2\sigma(T + 1)\right. \tag{73}$$

$$-\sigma\gamma + T\sigma\gamma - \sigma^2\gamma T - \sigma^2\gamma) + 2X^2\sigma^2(T + 1) = 0, \tag{74}$$

$$\lambda^4 + \lambda^3(2\sigma + 1 - \gamma) + \lambda^2 + \left[\frac{-\gamma R}{T + 1} + 2\sigma(1 - \gamma) + \sigma(\sigma - 1)(T + 1)\right]\lambda^2 \tag{75}$$

$$+\left[\frac{-2\sigma\gamma R}{T + 1} + \sigma\gamma(2 - \sigma)(T + 1) - R\right]\lambda + 2\sigma^2 Y(T + 1 - R) = 0, \tag{76}$$

$$\frac{\sigma\gamma^2(T + 3)(1 - \gamma - \sigma - \sigma T)}{(T + 1)^2}R^2 - \sigma\gamma\left[(2\sigma + 1 - \gamma)\{\gamma(2 - \sigma) + \frac{2\sigma(1 - \gamma)(T + 3)}{T + 1}\right. \tag{77}$$

$$+\sigma(T + 3)(\sigma - 1) - 2\sigma(2\sigma + 1 - \gamma)\} - 2\sigma\gamma(T + 3)(2 - \sigma)]R, \tag{78}$$

$$+\sigma^2\gamma(T + 1)(2 - \sigma)[(2\sigma + 1 - \gamma)2(1 - \gamma) + (1 - \sigma)(T + 1) - \gamma(T + 1)(2 - \sigma)] = 0. \tag{79}$$

The loss of stability of the convection fixed points for $\sigma = 10, \gamma = -\frac{8}{3}$ using Eq. (80) is evaluated to be $R_{c2} = 25.75590$ for system parameters T = 0, R_{c2} for T = 0.1, $R_{c2} = 25.75590$ for T = 0.2, $R_{c2} = 29.344020$ for T = 0.45, and $R_{c2} = 32.775550$ for T = 0.6.

5.1 Nusselt number

According to our problem, the horizontally averaged Nusselt number for an oscillatory mode of convection is given by

$$\mathrm{Nu}(\tau) = \frac{conduction + convection}{conduction}. \tag{80}$$

$$= \frac{\left[\frac{a}{2\pi}\int_0^{\frac{2\pi}{a_c}}\left(\frac{\partial T_b}{\partial z} + \frac{\partial T_2}{\partial z}\right)dx\right]_{z=0}}{\left[\frac{a_c}{2\pi}\int_0^{\frac{2\pi}{a_c}}\left(\frac{\partial T_b}{\partial z}\right)dx\right]_{z=0}}. \tag{81}$$

$$= 1 + \frac{\left[\frac{a}{2\pi}\int_0^{\frac{2\pi}{a_c}}\left(\frac{\partial T_2}{\partial z}\right)dx\right]_{z=0}}{\left[\frac{a_c}{2\pi}\int_0^{\frac{2\pi}{a_c}}\left(\frac{\partial T_b}{\partial z}\right)dx\right]_{z=0}}. \tag{82}$$

In the absence of the fluid motions, the Nusselt number is equal to 1. And simplifying the above equation, we will get the expressions for heat transfer coefficient:

$$\mathrm{Nu} = 1 - 2\pi B_2(\tau). \tag{83}$$

6. Result and discussion

In this section we present some numerical simulation of the system of Eqs. (62)–(65) for the time domain $0 \leq \tau \leq 40$. The computational calculations are obtained by using Mathematica 17, fixing the values $\sigma = 10, \gamma = -8/3,$ and taking in the initial conditions X(0) = Y(0) = 0.8, Z(0) = 0.9. In the case of T = 0, it is found that at $R_{c^1} = 1$, obtained from Eq. (80), the motionless solution loses stability, and the convection solution occurs. Also the eigenvalues from Eq. (80) become equal and complex conjugate when R varies from 24.73684209 to 34.90344691 given by Gupta et al. [28]. The evolution of trajectories over a time domain in the state space for increasing the values of scaled Rayleigh number and modulation terms is given in the figures. The projections of trajectories onto Y-X, Z-Y, Z-Y, and W-Z planes are also drawn (**Figure 1**). In **Figure 2**, we observe that the trajectory moves to the steady convection points on a straight line for a Rayleigh number (R = 1:1) just above motionless solutions. It is clear from **Figure 3a** that the trajectories of the solutions approach the fixed points at R = 12, which means the motionless solution is moving around the fixed points. As the value of R changes around R = 25.75590, there is a sudden change and transition to chaotic solution (in **Figure 3b**).

In the case of gravity modulation in **Figure 4**, just keeping the values $\delta_g = 0.05, \omega_g = 10$ in connection with **Figure 3**, the motionless solution loses stability, and convection solution takes over. Even at the subcritical value of R = 25.75590, transition to chaotic behavior solution occurs, but one can develop fully chaotic nature with suitably adjusting the modulation parameter values $\delta_g = 0.05, \omega_g = 10$.

To see the effect of rotation on chaotic convection for the value of T = 0.45, we get $R_{c^1} = 1.45$ from Eq. (80), which concludes that the motionless solution loses stability at this stage and the convection solution takes over. The other second and third eigenvalues become equal and complex conjugate at R = 31.44507647. In this state the convection points lose their stability and move onto the chaotic solution. The corresponding projections of trajectories and evolution of trajectories are presented in **Figure 5a** and **b**, planes Y-X, Z-X, Z-Y, and W-Z. At the subcritical value of R = 31.44507647, transition to chaotic behavior solution occurs. Observing **Figure 5b** it is clearly evident that in the presence of modulation $\sigma = 20, \delta_g = 0.2,$

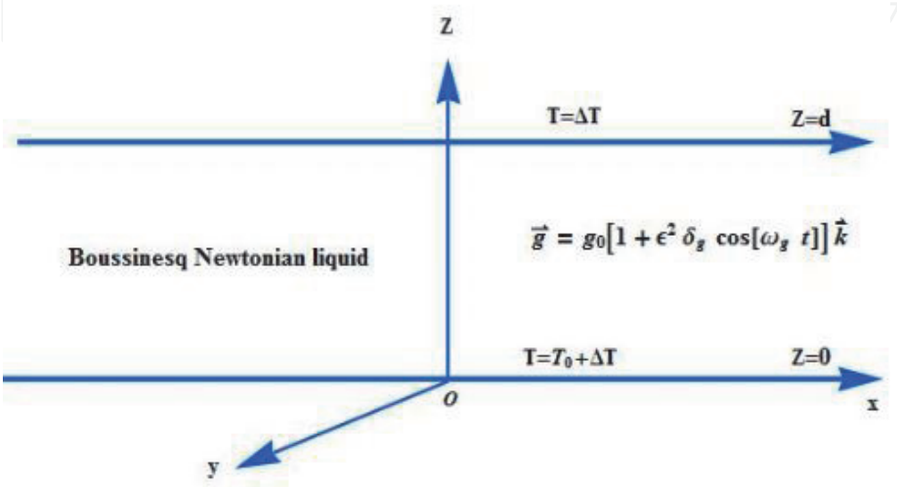

Figure 1.
Physical configuration of the problem.

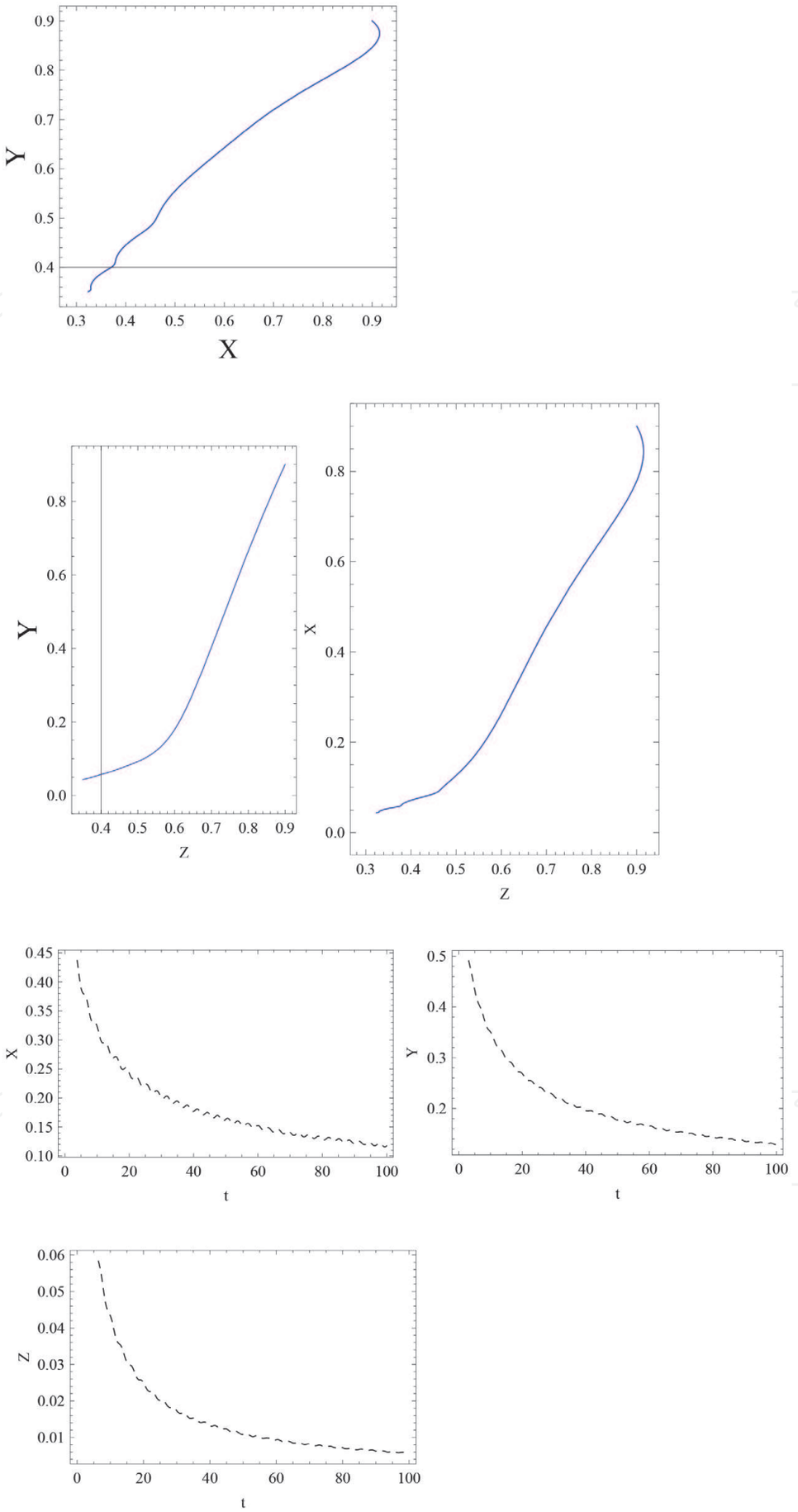

Figure 2.
Phase portraits for the evolution of trajectories over time in the state space for increasing the value of rescaled Rayleigh number (R). The graphs represent the projection of the solution data points onto Y-X, Z-X, Z-Y, and W-Z planes for $\gamma = -8/3$; $\sigma = 10$, $T = 0.1$, $R = 1.1$ $\omega_g = 0$, $\delta_g = 0.0$.

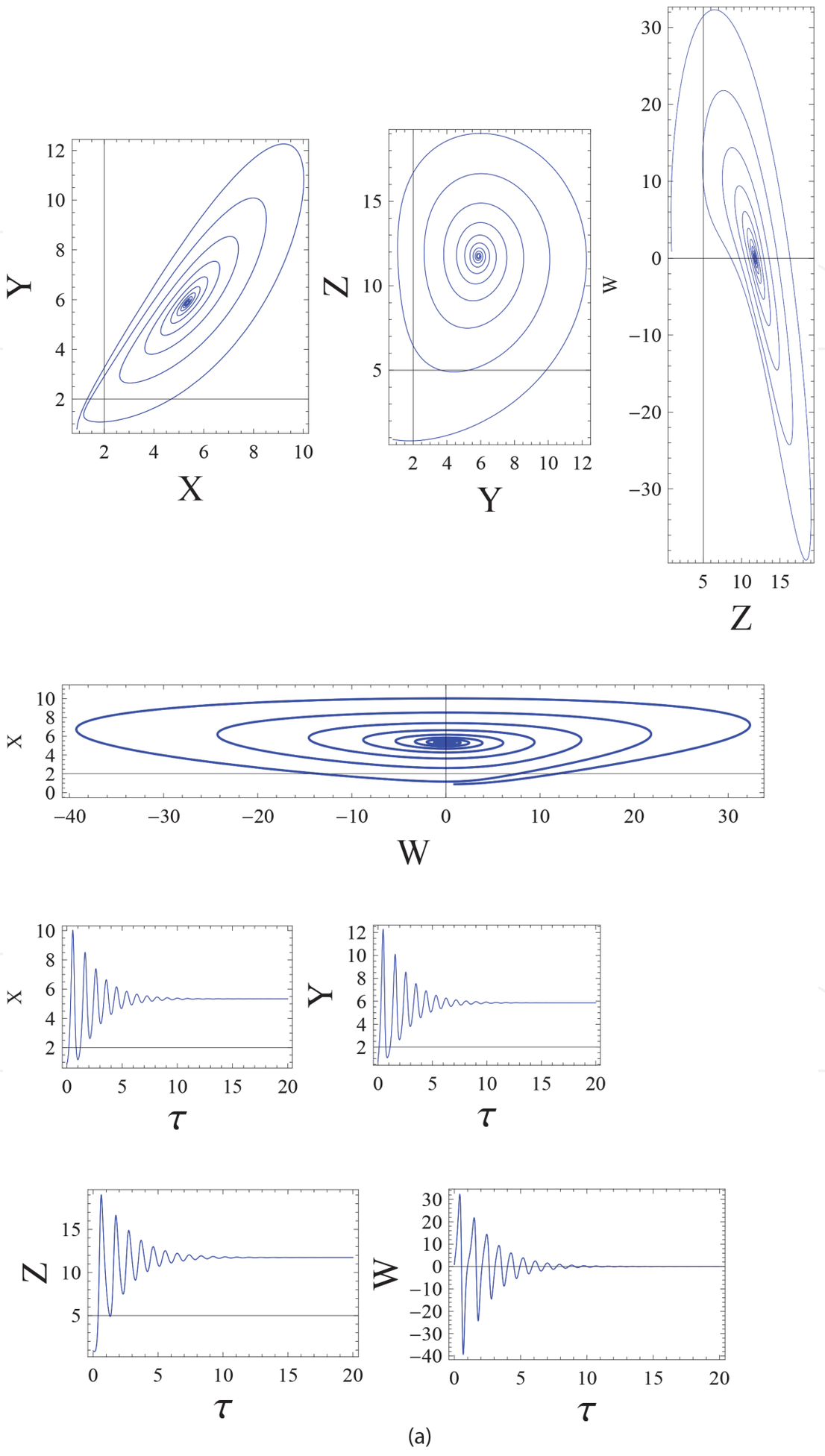

(a)

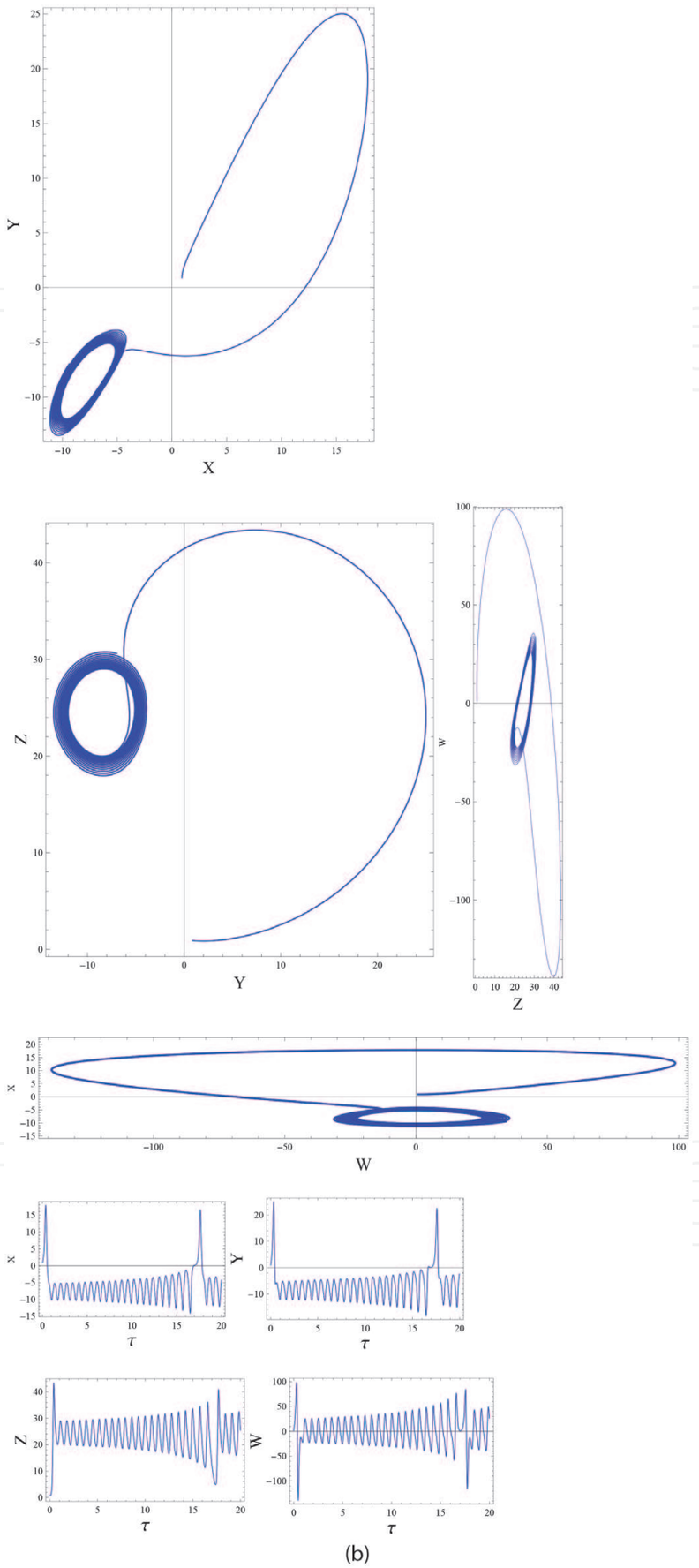

Figure 3.
(a) Phase portraits for the evolution of trajectories over time in the state space Y-X, Z-X, Z-Y, and W-Z planes for $\gamma = -8/3$, $\sigma = 10, T = 0.1$, $R = 12$, $\omega_g = 2$, $\delta_g = 0.0$. *(b) Phase portraits for the evolution of trajectories over time in the state space Y-X, Z-X, Z-Y, and W-Z planes for* $\gamma = -8/3$, $\sigma = 10, T = 0.1$, $R = 25.75590$, $\omega_g = 2$, $\delta_g = 0.0$.

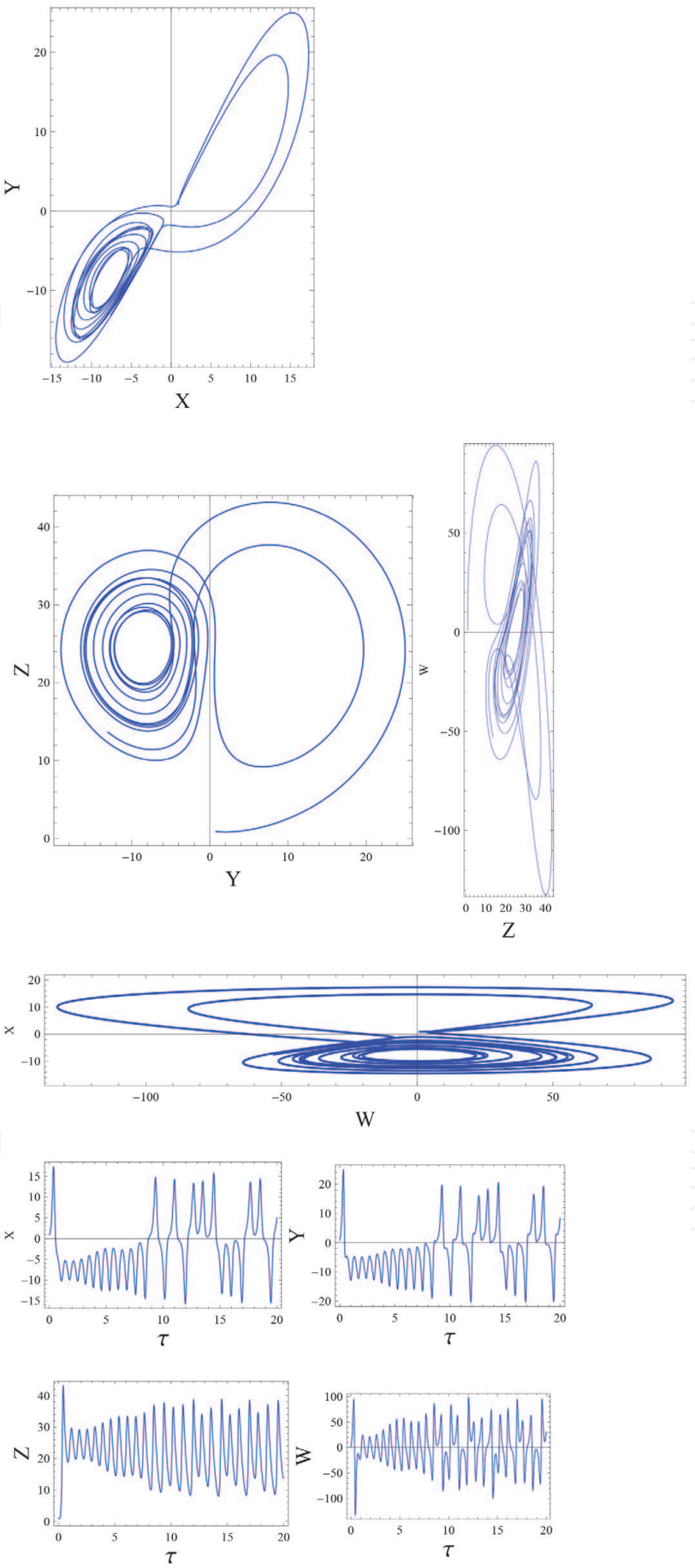

Figure 4.
Phase portraits for the evolution of trajectories over time in the state space modulation. The graphs represent the projection of the solution data points onto Y-X, Z-X, Z-Y, and W-Z planes for $\gamma = -8/3$; $\sigma = 10$, $T = 0.1$, $R = 1.1$, $\omega_g = 10$, $\delta_g = 0.05$.

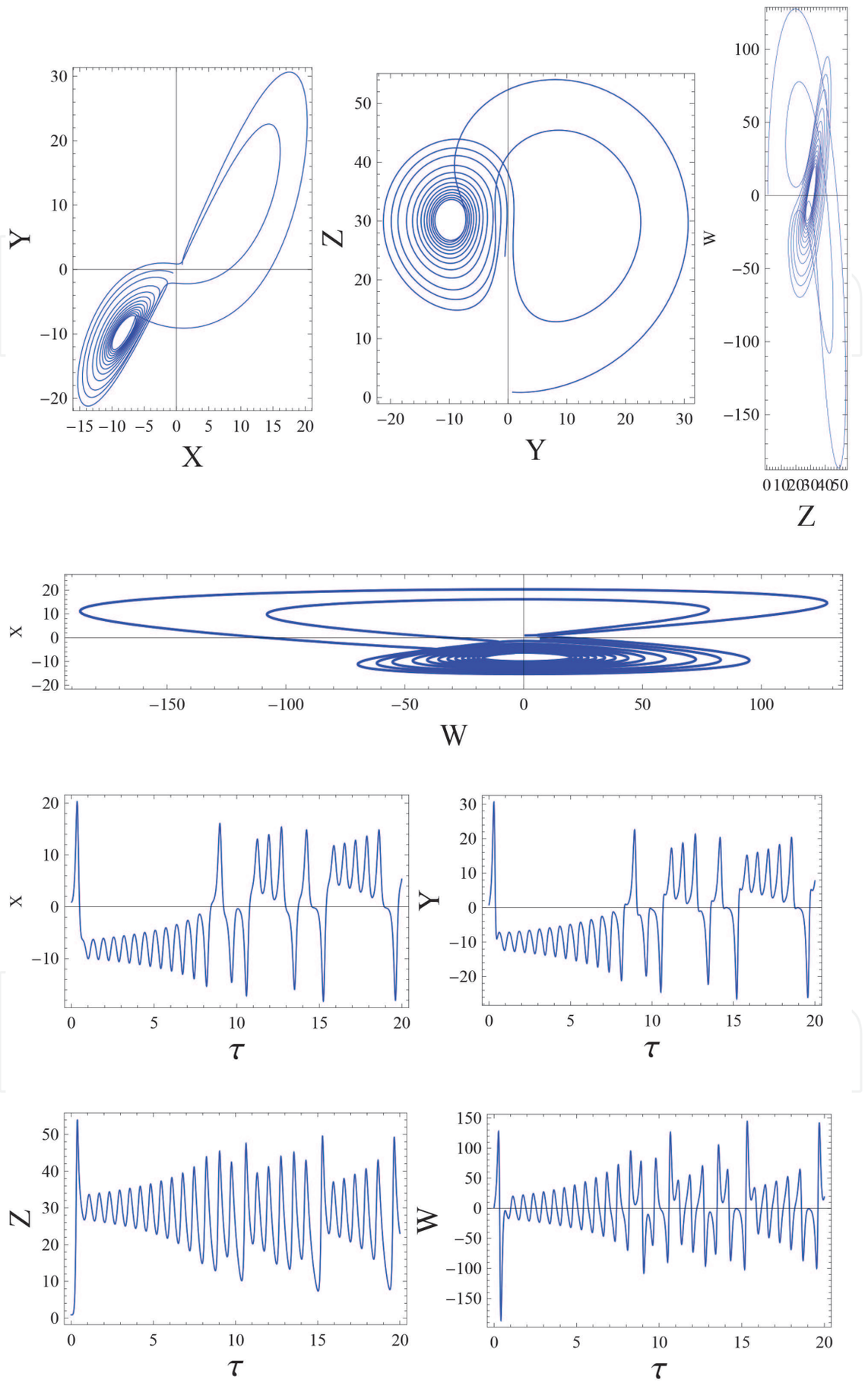

(a)

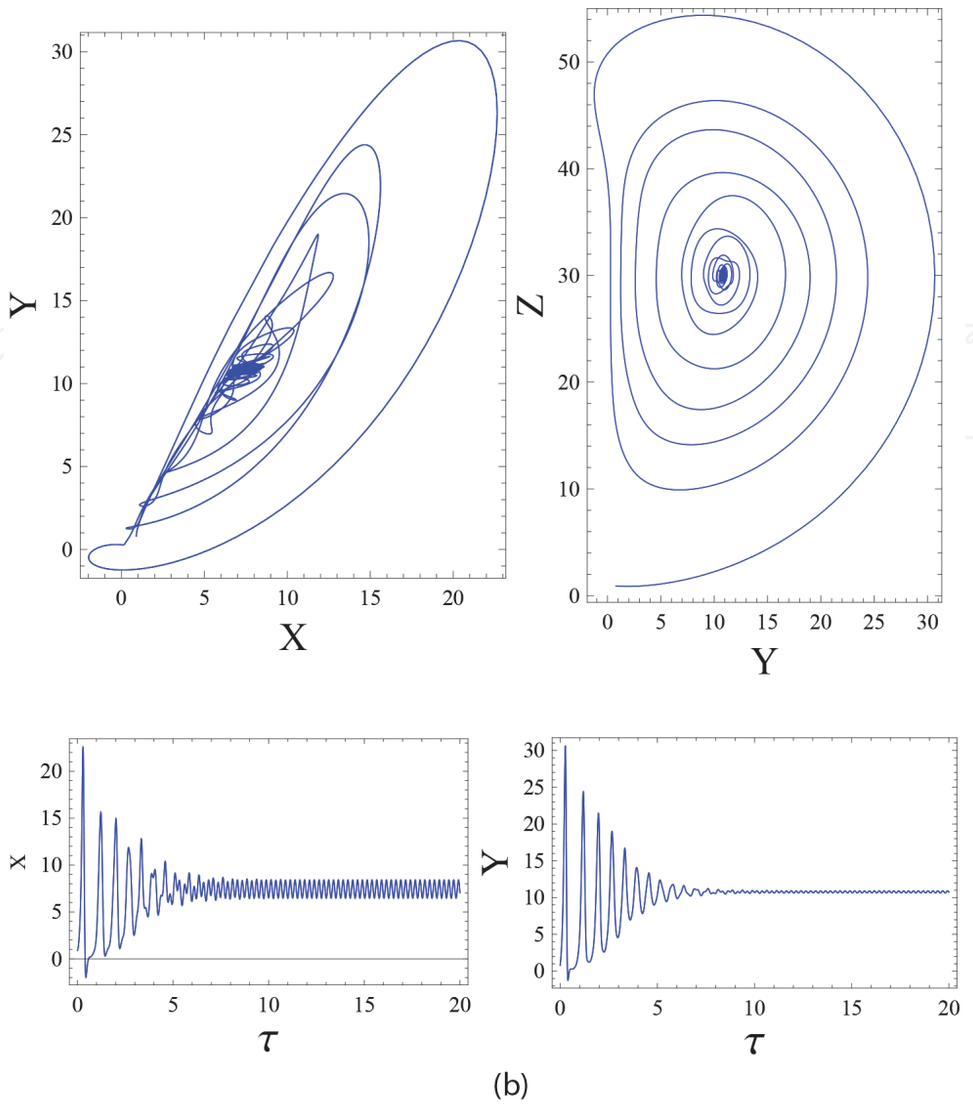

Figure 5.
(a) Phase portraits for the evolution of trajectories over time in the state space Y-X, Z-X, Z-Y, and W-Z planes for $\gamma = -8/3$, $\sigma = 10, T = 0.2$, $R = 31.44507647$, $\omega_g = 2$, $\delta_g = 0.0$. *(b) Phase portraits for the evolution of trajectories over time in the state space Y-X and Z-Y planes for* $\gamma = -8/3$, $\sigma = 20, T = 0.2$, $R = 31.44507647$, $\omega_g = 25$, $\delta_g = 0.2$.

$\omega_g = 20$, the trajectories are manifolds around the fixed points. Which are the interesting results to see that the system is unstable mode with rotation and buoyancy. But with gravity modulation, the system becomes stable mode.

For the value of T = 0.6, we obtain the motionless solution (where the system loss stability) given in **Figure 5b**. The values of the second and third eigenvalues become equal and complex conjugate when the value of R = 24.73684209; at this point the convection points lose their stability, and chaotic solution must occur. But due to the presence of modulation, the trend is reversed given in **Figure 6**. Observing that in the presence of modulation $\delta_g = 0.1, \omega_g = 2$, the system will come to stable mode for large values of R. The effect of frequency of modulation for the values $\omega_g = 2$ and $\omega_g = 20$ on chaos is presented in **Figure 7a** and **b**. It is clear that low-frequency-modulated fluid layer is in stable mode and high-frequency-modulated fluid layer in unstable mode. The reader may have look on the studies of [29–33] for the results corresponding to the modulation effect on chaotic convection.

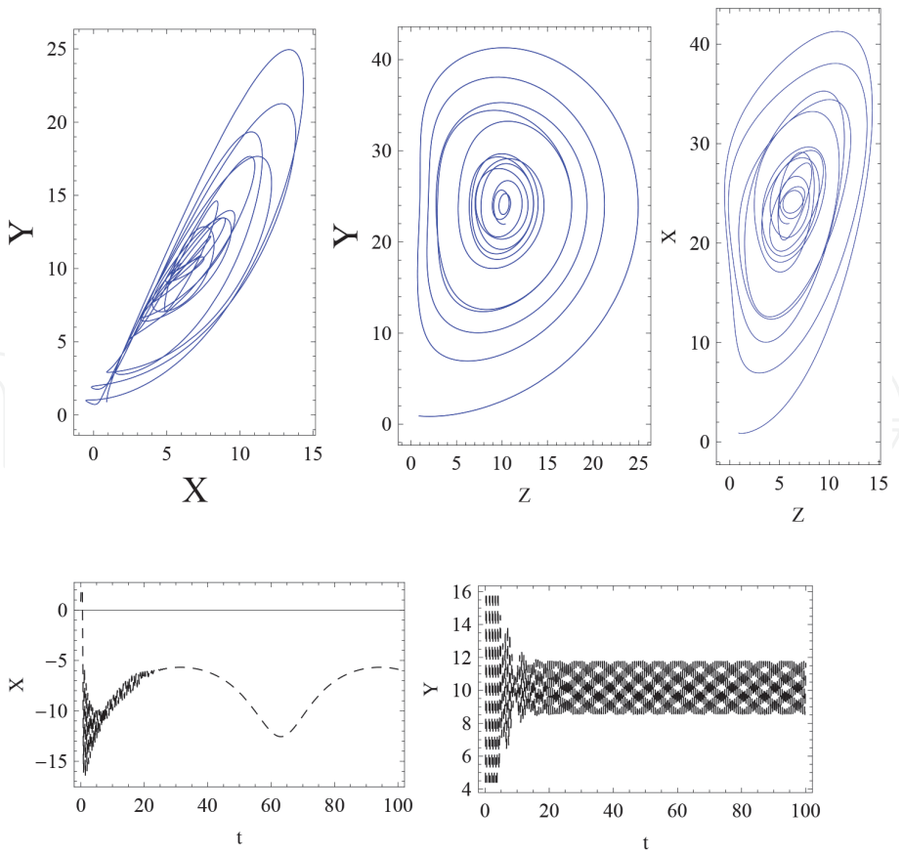

Figure 6.
Phase portraits for the evolution of trajectories over time in the state space Y-X and Z-Y planes for $\gamma = -8/3$, $\sigma = 20, T = 0.6, R = 24.73684209, \omega_g = 10, \delta_g = 0.1$.

Finally we also derived the heat transfer coefficient (Nu(τ)) given by Eq. (83) and verified the rate of transfer of heat under the effect of gravity modulation. It is clear from **Figure 8** that heat transfer in the system is high for low-frequency modulation and for δ_g values varies from 0.1 to 0.5. The results corresponding to the gravity modulation may be observed with the studies of [19–26].

7. Conclusions

In this chapter, we have studied chaotic convection in the presence of rotation and gravity modulation in a rotating fluid layer. It is found that chaotic behavior can be controlled not only by Rayleigh or Taylor numbers but by gravity modulation. The following conclusions are made from the previous analysis:

1. The gravity modulation is to delay the chaotic convection.

2. Taking the suitable ranges of ω_g, δ_g, and R, the nonlinearity is controlled.

3. The chaos in the system are controlled by gravity modulation either from stable to unstable or unstable to stable depending on the suitable adjustment of the parameter values.

4. The results corresponding to g-jitter may be compared with Vadasz et al. [27], Kiran [31] and Bhadauria and Kiran [33].

5. It is found that heat transfer is enhanced by amplitude of modulation and reduced by frequency of modulation.

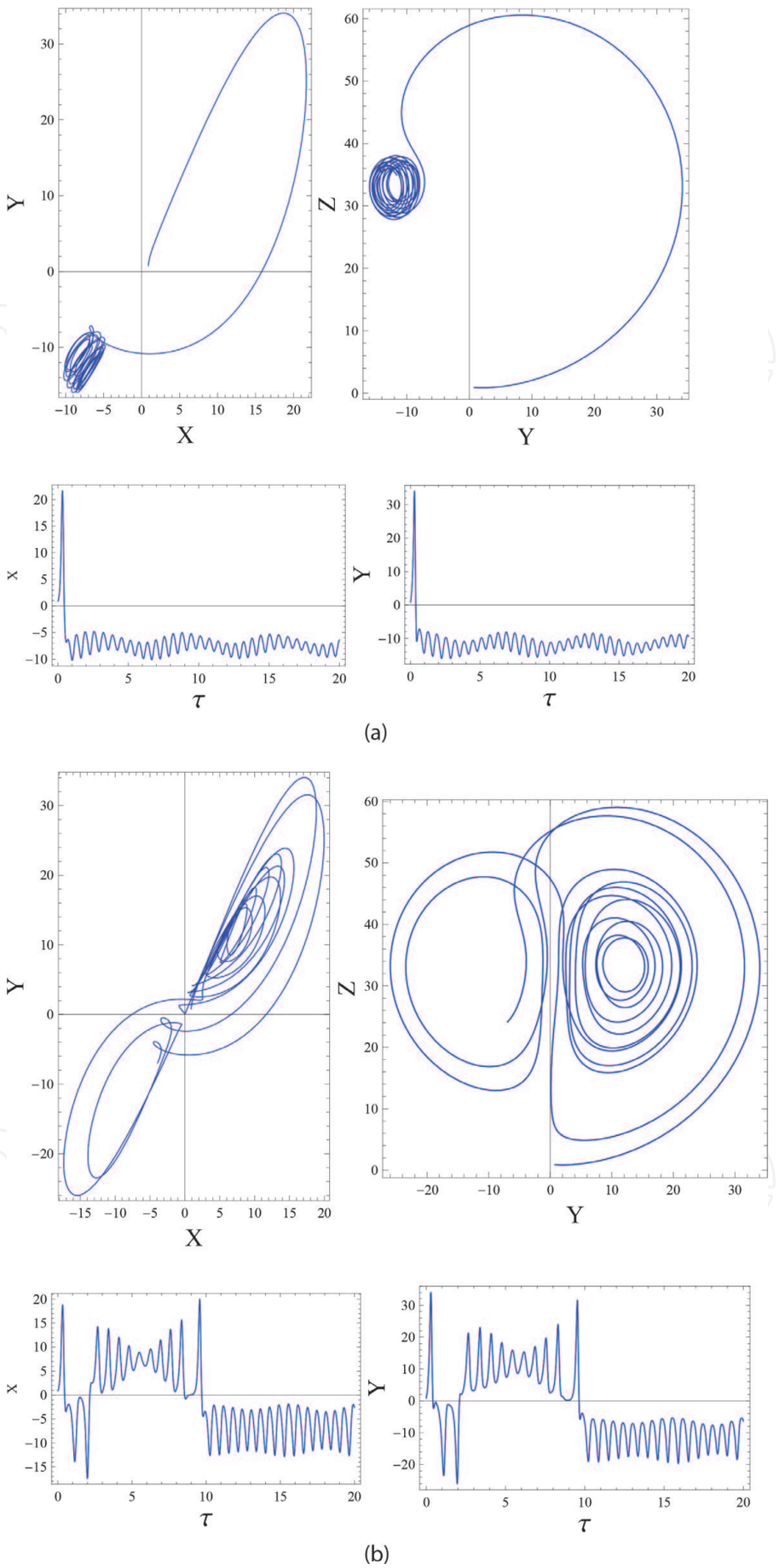

Figure 7.
(a) For γ = −8/3, σ = 20, T = 0.2, R = 34.90344691, ω_g = 2, δ_g = 0.1. (b) Phase portraits for the evolution of trajectories over time in the state space Y-X and Z-Y planes for γ = −8/3, σ = 20, T = 0.2, R = 34.90344691, ω_g = 20, δ_g = 0.1.

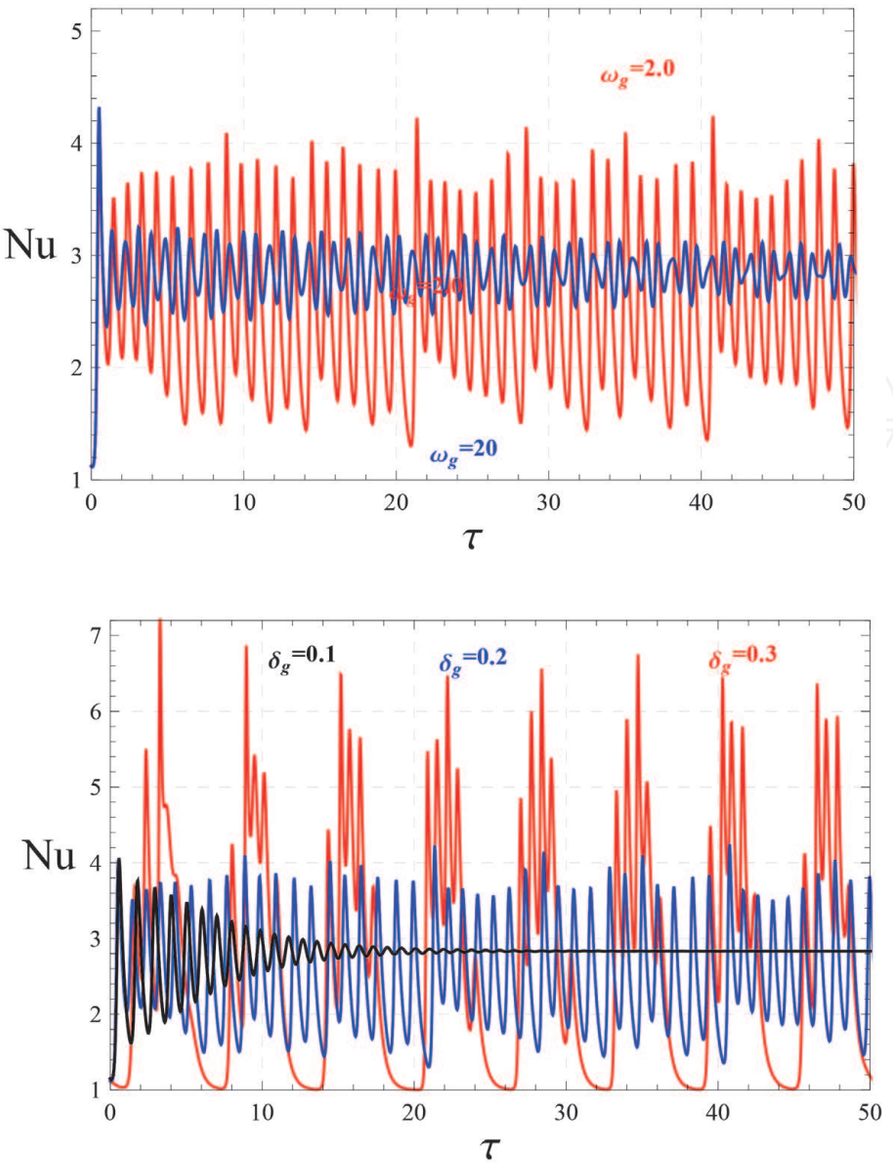

Figure 8.
Effect of ω_g and δ_g on Nu.

Acknowledgements

The author Palle Kiran is grateful to the college of CBIT for providing research specialties in the department. He also would like to thank Smt. D. Sandhya Shree (Board member of CBIT) for her encouragement towards the research. He also would like to thank the HOD Prof. Raja Reddy, Dept. of Mathematics, CBIT, for his support and encouragement. Finally the author PK is grateful to the referees for their most valuable comments that improved the chapter considerably.

Conflict of interest

The authors declare no conflict of interest.

Author details

Palle Kiran
Department of Mathematics, Chaitanya Bharathi Institute of Technology, Hyderabad, Telangana, India

*Address all correspondence to: pallkiran_maths@cbit.ac.in

References

[1] Lorenz EN. Deterministic non-periodic flow. Journal of Atmospheric Sciences. 1963;**20**:130-142

[2] Venezian G. Effect of modulation on the onset of thermal convection. Journal of Fluid Mechanics. 1969;**35**:243-254

[3] Gresho PM, Sani RL. The effects of gravity modulation on the stability of a heated fluid layer. Journal of Fluid Mechanics. 1970;**40**:783-806

[4] Bhadauria BS, Kiran P. Weak nonlinear oscillatory convection in a viscoelastic fluid saturated porous medium under gravity modulation. Transport in Porous Media. 2014; **104**(3):451-467

[5] Bhadauria BS, Kiran P. Weak nonlinear oscillatory convection in a viscoelastic fluid layer under gravity modulation. International Journal of Non-Linear Mechanics. 2014; **65**:133-140

[6] Donnelly RJ. Experiments on the stability of viscous flow between rotating cylinders III: Enhancement of hydrodynamic stability by modulation. Proceedings of the Royal Society of London. Series A, Mathematical and Physical Sciences. 1964;**A281**:130-139

[7] Kiran P, Bhadauria BS. Weakly nonlinear oscillatory convection in a rotating fluid layer under temperature modulation. Journal of Heat Transfer. 2016;**138**(5):051702

[8] Bhadauria BS, Suthar OP. Effect of thermal modulation on the onset of centrifugally driven convection in a vertical rotating porous layer placed far away from the axis of rotation. Journal of Porous Media. 2009;**12**(3):239-252

[9] Bhadauria BS, Kiran P. Weak nonlinear analysis of magneto–convection under magnetic field modulation. Physica Scripta. 2014; **89**(9):095209

[10] Chen GR, Ueta T. Yet another chaotic attractor. International Journal of Bifurcation and Chaos. 1999;**9**:1465-1466

[11] Vadasz P, Olek S. Weak turbulence and chaos for low Prandtl number gravity driven convection in porous media. Transport in Porous Media. 1999; **37**:69-91

[12] Vadasz P. Local and global transitions to chaos and hysteresis in a porous layer heated from below. Transport in Porous Media. 1999;**37**: 213-245

[13] Mahmud MN, Hasim I. Effect of magnetic field on chaotic convection in fluid layer heated from below. International Communications in Heat and Mass Transfer. 2011;**38**: 481-486

[14] Feki M. An adaptive feedback control of linearizable chaotic systems. Chaos, Solitons and Fractals. 2003;**15**: 883-890

[15] Yau HT, Chen CK, Chen CL. Sliding mode control of chaotic systems with uncertainties. International Journal of Bifurcation and Chaos. 2000;**10**: 113-1147

[16] Sheu LJ, Tam LM, Chen JH, Chen HK, Kuang-Tai L, Yuan K. Chaotic convection of viscoelastic fluids in porous media. Chaos, Solitons and Fractals. 2008;**37**:113-124

[17] Vadasz P. Analytical prediction of the transition to chaos in Lorenz equations. Applied Mathematics Letters. 2010;**23**:503-507

[18] Narayana M, Gaikwad SN, Sibanda P, Malge RE. Double diffusive magneto-convection in viscoelastic

fluids. International Journal of Heat and Mass Transfer. 2013;**67**:194-201

[19] Kirna P. Nonlinear throughflow and internal heating effects on vibrating porous medium. Alexandria Engineering Journal. 2016;**55**(2):757-767

[20] Kirna P, Manjula SH, Narasimhulu Y. Oscillatory convection in a rotating fluid layer under gravity modulation. Journal of Emerging Technologies and Innovative Research. 2018;**5**(8):227-242

[21] Kirna P, Narasimhulu Y. Centrifugally driven convection in a nanofluid saturated rotating porous medium with modulation. Journal of Nanofluids. 2017;**6**(1):01-11

[22] Kirna P, Bhadauria BS. Throughflow and rotational effects on oscillatory convection with modulated. Nonlinear Studies. 2016;**23**(3):439-455

[23] Kirna P, Narasimhulu Y. Weakly nonlinear oscillatory convection in an electrically conduction fluid layer under gravity modulation. International Journal of Applied Mathematics and Computer Science. 2017;**3**(3):1969-1983

[24] Kirna P, Bhadauria BS, Kumar V. Thermal convection in a nanofluid saturated porous medium with internal heating and gravity modulation. Journal of Nanofluids. 2016;**5**:01-12

[25] Kiran P. Throughow and g-jitter effects on binary fluid saturated porous medium. Applied Mathematics and Mechanics. 2015;**36**(10):1285-1304

[26] Vadasz JJ, Meyer JP, Govender S. Chaotic and periodic natural convection for moderate and high prandtl numbers in a porous layer subject to vibrations. Transport in Porous Media. 2014;**103**: 279-294

[27] Kiran P, Bhadauria BS. Chaotic convection in a porous medium under temperature modulation. Transp Porous Media. 2015;**107**:745-4763

[28] Gupta VK, Bhadauria BS, Hasim I, Jawdat J, Singh AK. Chaotic convection in a rotating fluid layer. Alexandria Engineering Journal. 2015;**54**:981-992

[29] Vadasz P, Olek S. Route to chaos for moderate Prandtl number convection in a porous layer heated from below. Transport in Porous Media. 2000;**41**: 211-239

[30] Kiran P, Narasimhulu Y. Internal heating and thermal modulation effects on chaotic convection in a porous medium. Journal of Nanofluids. 2018; **7**(3):544-555

[31] Kiran P. Vibrational effect on internal heated porous medium in the presence of chaos. International Journal of Petrochemical Science & Engineering. 2019;**4**(1):13-23

[32] Kirna P, Bhadauria BS. Chaotic convection in a porous medium under temperature modulation. Transport in Porous Media. 2015;**107**:745-763

[33] Bhadauria BS, Kiran P. Chaotic and oscillatory magneto-convection in a binary viscoelastic fluid under G-jitter. International Journal of Heat and Mass Transfer. 2015;**84**:610-624